Environmental Advances 7 (2022) 100158

Contents lists available at ScienceDirect

Environmental Advances

journal homepage: www.sciencedirect.com/journal/environmental-advances

Mechanisms of emerging contaminants removal by novel neem chip biochar

Thusalini Manoharan [a], Sashikesh Ganeshalingam [b], Kannan Nadarajah [a,*]

[a] Department of Agricultural Engineering, Faculty of Agriculture, University of Jaffna, Sri Lanka
[b] Department of Chemistry, Faculty of Science, University of Jaffna, Sri Lanka

ARTICLE INFO

Keywords:
Biochar
Emerging contaminant
Isotherm
Kinetics
Mancozeb
Neem
Pyrolysis
Surface science
Thermodynamics

ABSTRACT

Emerging contaminants (ECs) play a vital role in water pollution. The treatment methods used for the removal are expensive and complex. It is therefore highly needed to develop cost-effective materials for the effective removal of ECs. This study comprehensively investigated the potential of biochar material pyrolyzed at different temperatures in removing mancozeb, a potential EC, reported to significantly pollute water sources in Sri Lanka. Detailed isotherm, kinetics, thermodynamics and rate-limiting factor analysis were performed for biochar with high adsorptive capacity along with FTIR and XRD characterization. Results revealed that biochar pyrolyzed at 900 °C exposed higher adsorptive performance of 187.68 mg/g. Moreover, a detailed isotherm study exhibited that the adsorption of mancozeb to biochar is multilayer in nature. The pseudo second-order equation is well fitted to explain the adsorption rate of mancozeb. In addition, the thermodynamic analysis explains that the adsorption is spontaneous and endothermic. The XRD information well explains the carbon network development with an increase in pyrolysis temperature. At higher pyrolysis temperatures, the constricted carbon network was formed. FTIR analysis expresses that the functional groups are degraded at higher pyrolysis temperature. The rate-limiting analysis indicates that the removal rate of mancozeb by biochar derived from neem chips pyrolyzed at 900 °C initially induced by mass diffusion followed by intraparticle diffusion. The innovative finding of the use of biochar produced from neem chip for the removal of mancozeb makes an opening to the development of noval strategies for the effective removal of ECs at the commercial level.

1. Introduction

ECs are either naturally or synthetically occurring chemical substances or any microorganisms that are uncommon in the environment, but can enter the atmosphere (Rosenfeld and Feng, 2011). ECs are usually found in all most all the products that are used daily basis and finally, those toxic components are released into the environment. ECs contain pesticides, pharmaceuticals, personal care products, industrial chemicals and surfactants which are continuously found in groundwater, drinking water, surface water, food sources and wastewater released via industrial and domestic activities. Furthermore, this type of contaminants comprises analgesics, endocrine-disrupting compounds, hormones, antibiotics and a range of pharmaceutical compounds comprising the drugs related to anti-inflammatory and antiepileptic effects (Rosenfeld and Feng, 2011).

Pesticides play a major role in the global agriculture system in recent years allowing for significant increases in crop yields and food supply. During the past three decades, the global usage of fungicides and bactericides has been increased by 140,000 tons (FAOSTAT, 2021). Pesticides exposure can occur directly through occupational exposure, like those who engaged in farm activity, or indirectly via environmental exposure to water, air, soil and through the ingestion of contaminated food which causes harm to the entire population (Weis et al., 2019). Due to runoff, sub-surface drainage, spray drift and leaching, pesticides reach the water bodies. Meanwhile, the metabolites of pesticide residues in water is considered biologically active, toxic and found in water at a higher level (Naidu et al., 2016). Fungicides are kinds of a pesticide, that restrict the growth of fungus and their spores. Generally, the fungicides are used in the field of agriculture to control the fungal causing plant diseases such as root rot, damping-off, rust, powdery mildew, downy mildew, etc.

Mancozeb belongs to the group of ethylene bis-dithiocarbamate (EBDC) fungicides, which was initially registered as a broad-spectrum fungicide in United States in 1948 (Runkle et al., 2017). Mancozeb

* Corresponding author.
E-mail address: aenkanna@gmail.com (K. Nadarajah).

https://doi.org/10.1016/j.envadv.2021.100158
Received 30 October 2021; Received in revised form 13 December 2021; Accepted 20 December 2021
Available online 28 December 2021

has been used as a fungicide in agriculture as well as industrial purposes for almost 70 years. According to market analysis, the selling of mancozeb was around $ 740 million in 2007 around the globe. In 2019, the market value of mancozeb was recorded as $ 795.4 million, and it is expected to achieve $ 832.8 million in 2026 (Angelo et al., 2010; MarketWatch News Department, 2021). Demand for mancozeb is getting increased in the world market due to its cheap purchasing price, rising worldwide demand for vegetables and fruits and non-selective fungicidal effectiveness (Runkle et al., 2017). Mancozeb can be easily degraded by heat, light and moisture, and it generates metabolites like ethylenethiourea (ETU) and ethylenebisisothiocyanate (EBIS). Mancozeb is categorized as a Class II or very hazardous chemical by the World Health Organization (WHO), and numerous studies have proved that mancozeb and its major metabolite, ethylenthiourea (ETU), to a range of health consequences including endocrine disruption, cancer and reproductive damage (Weis et al., 2019).

There are various modern techniques and treatment technologies available for the removal of contaminants such as processes of phase-changing (Homem and Santos, 2011), advanced oxidation processes (Khan et al., 2020), biological treatment and adsorption in different solid membranes and matrices that have been extensively practiced to remove the micro-pollutants (Rodriguez-Narvaez et al., 2017). In tertiary treatment systems, coagulation, flocculation, ozonation, lamellar settlement, chlorination and filtration are practiced to remove the ECs (Matamoros and Salvadó, 2013). Among all treatment processes, adsorption can be characterized as one of the promising methods globally for the removal of ECs. The use of low-cost biochar adsorbents to remove organic and inorganic contaminants present in an aqueous solution will be a comparatively more profitable way than the traditional methods for the removal of the contaminants from water.

Biochar is a solid material rich in carbon produced from the process of pyrolysis of any biomass under the oxygen-limiting environment (Keerthanan et al., 2020). Based on previous researches, it is clear that a variety of low-cost, effective, composite , modified biochar could adsorb emerging contaminants from the wastewater (Li et al., 2019). Neem (*Azadirachta indica*) which is a tree species belongs to the family Meliaceae. Neem bark consists of 65.63% of cellulose, 23.55% of hemicellulose and 9.04% of lignin (Al-Eraky et al., 2016). These components play a major role in the determination of biochar characters during pyrolysis. It is very common in Asian contries with medicinal properties. There are amble researches available in literatature to remove pollutants from aqueous solution using neem. For instant, Pb^{2+} was removed using mature leaves of the Neem (Azadirachta indica), and neem saw dust was used as biosorbants (Bhattacharyya and Sharma, 2004; Naiya et al., 2008). Bhattacharyya and Sharma investigaded the thermodynamic and kinetics of methylene blue adsorption on neem leaf powder (Bhattacharyya and Sharma, 2005). Mandal et al., reported the use of neem leaves powder as a biosorbent in the removal of phenolic componads from the wastewater (Mandal et al., 2020). Futhermore biochar derived from neem leaves were also used to remove the hexavalent chromium (Thangagiri et al., 2022). From the literature, there is an evident that different parts of neem tree were used as biosorbent and for the preparation of biochar. However, the use of neem chip for biochar preparation is still not known well.

This study is the first report to investigate the feasibility of neem (*Azadirachta indica*) chip biochar to remove mancozeb from an aqueous solution by the comprehensive understanding of adsorption mechanism. There are ample researches carried out to determine the use of neem leaves, seeds and husks as biosorbents and as biochar except neem chips to remove different contaminants (Cr^{2+}, Pb^{2+}, Methyl Blue, etc.). However, the use of such materials for mancozeb is highly limited. Therefore, it is well clear that the use of neem chip biochar for the removal of mancozeb is an innovative technique to reduce the contaminants in the wastewater. Furthermore, the findings related to kinetics and thermodynamics of neem chip biocharat different temperatures, pH and incubation periods could be useful to formulate novel techniques for the adsorption of mancozeb, and it can add new knowledge to the adsorption science. Moreover, this comprehensive work directs future research openings for the development of activated carbon materials from novel neem chip biochar with enhanced adsorptive performances for different ECs.

2. Materials and methods

2.1. Materials

Commercial grade Mancozeb [80% (W/W)] was purchased at a commercial agriculture shop located in Paranthan, Sri Lanka. Neem timber was collected at a local carpentry shop at Thirukkovil, Sri Lanka. Mancozeb stock solution was prepared by dissolving mancozeb powder with 25 mM Alkaline EDTA solution (Petha et al., 2017). The calibration curve for mancozeb is given in Fig. S1.

2.2. Biochar production

Neem timber which was collected from a local carpentry shop, Thirukkovil, was copped and broken by hammer and chisel. The broken chips were first sieved by a 2 mm pore size sieve and the passed materials were sieved by a 1 mm pore size sieve. Finally, neem chip with size ranging from 1 to 2 mm was obtained. Neem chips were filled into ceramic crucibles with lid, and they were treated at 300, 500, 700 and 900 °C with a heating rate of 52.8°C min^{-1} for 2 h using muffle furnace (PC442T, Protherm furnace, Turkey). The obtained biochars were labeled as NBC300, NBC500, NBC700 and NBC900 respectively.

2.3. Biochar characterization

The yield of the biochar was determined by calculating the ratio between the weight of neem biochar and the weight of biomass (Keerthanan et al., 2020). The surface functional group was analyzed using Fourier Transform Infrared spectrophotometer (ALPHA II, BRUKER, Germany) coupled with ATR (attenuated total reflectance) mode with zinc selenide crystal. Spectra were collected within the spectral range of 4000 to 600 cm^{-1} with a resolution of 4 cm^{-1} using 32 average scans. Point zero charge (pzc) of biochar was determined by pH drift method (Nadarajah et al., 2021). In brief, accurately weighted 0.2 g of biochar pyrolyzed at different temperatures was added with 20 mL of NaCl solution at different pH values separately. Prepared solutions were placed into the shaking incubator (BSD-250, Boxun, Shanghai, China) for 24 h at 25 °C and 150 rpm. Final pH was determined after 24 h using multimeter (HQ40d, HACH, United Kingdom). The pzc was determined by a point where final pH and initial pH values are equal. Crystallographic features of biochars pyrolyzed at different temperatures were analyzed using X-ray diffraction (XRD) spectroscopy (AERIS, PANalytical, United Kingdom). Powdered samples were used for XRD analysis.

2.4. Adsorption experiment

Batch adsorption experiments were conducted for biochar pyrolyzed at different temperatures in 25 mL flat bottom glass bottles containing 20 mL of known concentration (200 mg/L) of mancozeb solution adjusted to desired pH (pH 5) with NaOH and HCl and added with the needed amount (1g/L) of Neem chip biochar. Each sample was placed into the shaking incubator (BSD-250, Boxun, Shanghai, China) operated at 150 rpm at 25 °C for 24 h. After 24 hours, solution was centrifuged with refrigerated centrifuge (Model: TGL-20) at 10000 rpm for 5 minutes. Then absorbance of the solution with appropriate dilution was measured by UV-vis spectrophotometer at 279 nm (UH5300 spectrophotometer, HITACHI, Japan). Three replicates were used for each experiment, and the average values were calculated.

The effect of biochar dosage on mancozeb removal was carried out at 25 °C with initial concentration of 200 mg/L at the pH 5, and the dosage

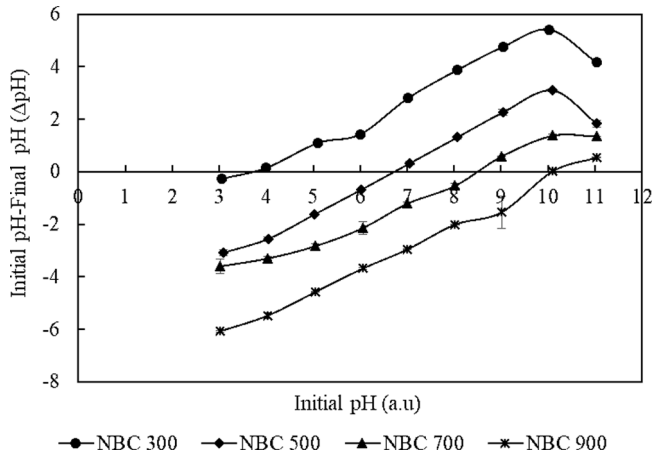

Fig. 1. pzc of NBC300, NBC500, NBC700 and NBC900

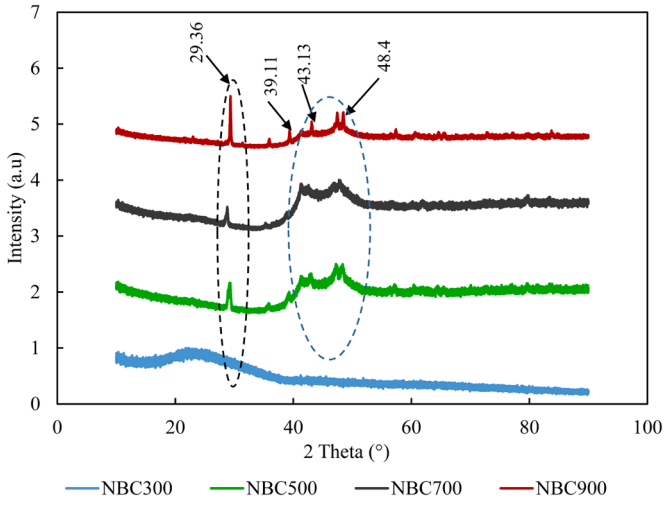

Fig. 2. XRD spectrum of neem biochar produced at different temperatures.

was set to range from 0.5 to 5 g/L. The effect of pH on mancozeb removal was studied using the initial dosage of 1g/L with pH ranging from 3 to 11 at 25 °C, and the influence of mancozeb concentration was assessed using 1 g/L initial dosage with concentration ranging from 100 to 500 mg/L at pH 5. The removal percentage and adsorptive capacity were measured by the Eqs. (1) and (2) respectively.

$$Removal\ \% = \frac{C_i - C_t}{C_i} \times\ 100 \tag{1}$$

$$q_e\ = \frac{V(C_i - C_t)}{W} \tag{2}$$

Where, q_e is the amount of adsorbate removed per g of adsorbent (adsorption capacity in mg/g), C_i is initial adsorbate concentration (mg/L), C_t is the adsorbate concentration (mg/L) in solution at time t (h), W is the biochar weight (g) and V is the solution volume (L).

2.5. Isotherm, kinetic, thermodynamics and rate-limiting factor analysis

Three different models were used to investigate the effect of adsorption rate and also to find the effect of equilibrium concentration on the adsorptive process. Models used were the pseudo first order kinetics, the pseudo second order kinetics and the Elovich. Adsorption isotherm studies were carried out using three models Langmuir, Freundlich and Temkin. Isotherm study was carried out to identify whether adsorption is monolayer or multilayer in nature. In addition, thermodynamics analysis was carried out at different temperatures of 25, 30 and 40 °C. Furthermore, Weber-Morris method was used to analyze the rate-limiting factor. The applicable equations for each model are given in Supplementary information.

3. Results and discussion

3.1. Biochar characterization

3.1.1. Effect of temperature

The effect of pyrolysis temperature on the yield of biochar produced from neem chips (Fig. S2) at different temperatures was studied. The yield of biochar decreased from 46.8% to 5.06% with an increase in pyrolysis temperature from 300 °C to 900 °C. The yields of biochar at 300 °C, 500 °C, 700 °C and 900 °C are 46.8%, 19.13%, 12.34%, and 5.06% respectively. There was a drastic reduction in yield from 300 °C to 500 °C. The yield reduction was due to the primary and secondary decomposition of biochar with an increase in temperature. The higher yield of 46.8% indicates that the partial pyrolysis had occurred at 300 °C. The yield reduction is mainly due to the destruction of components like hemicellulose and cellulose as well as diffusion of some organic matters at high pyrolysis temperature (Al-Wabel et al., 2013). In addition, higher yield recovery was due to lower losses of H_2, CH_4, and CO and lower condensation of aliphatic compounds (Novak et al., 2009). The yield reduction with increasing pyrolysis temperature matches with the result obtained from biochar derived from various biomass from plant, animal and human wastes (Shinogi and Kanri, 2003).

Neem bark consists of 65.63% of cellulose, 23.55% of hemicellulose, and 9.04% of lignin (Al-Eraky et al., 2016). These components play a major role in the determination of biochar chracteristics during pyrolysis. The cellulose molecule is a crystalline, solid, hydrolysis resistant polymer made up of glucose units with no branches (Al-Wabel et al., 2013). Hemicellulose, on the other hand, has spontaneous, amorphous compounds with little intensity. A dilute acid or base is having the ability to hydrolyze it quickly. Cross-linking can be used to create lignin. The big lignin molecules occupy three dimensions and are strongly cross-linked. In the case of thermal degradation, hemicellulose degrades first followed by cellulose and lignin (Al-Wabel et al., 2013). It had been reported that the moisture evolution had occurred at 220 °C, whereas hemicellulose degraded at temperatures from 220 to 300 °C, cellulose degraded at 340 °C and lignin degraded at the higher temperatures of 400 °C and above (Al-Wabel et al., 2013).

3.1.2. Surface charge distribution

Changes in point zero charges (pzc) obtained using pH drift method of different biochar illustrated in Fig. 1. The pzc is the point where the net charge of the biochar is equal to zero (Banik et al., 2018). Biochars , pyrolyzed at different temperatures, show different pzc values. The pzc values are getting increased with increasing pyrolysis temperatures. The pzc values of NBC 300, NBC500, NBC700 and NBC900 are 4, 7.06, 9.01 and 10.1 respectively. The pH of the equilibrated aqueous phase increases with an increase in salt concentration since NaCl solutions were used for the pzc measurements. When Na^+ competes with H^+ for negatively charged surface sites on the biochar, Cl^- competes with OH^- for positively charged surface sites on the biochar. It has been reported that the pzc value showed the linear increasing trend with increasing temperature (Banik et al., 2018). This is due to the biochars pyrolyzed at higher temperatures are with low concentrations of carboxylate groups and high concentrations of oxonium groups. Furthermore, this increasing trend indicates that the basic groups of biochar increase with pyrolysis temperature. The basic group indicates the occurrence of positive charge on the surface of biochar (Tran et al., 2016). When the pH of the solution is greater than the pzc value, the surface charge of biochar is negative and facilitates the adsorption of cations. In contrast, when the pH of the solution is lesser than the pzc value, the surface charge of biochar is positive and facilitates the adsorption of anions

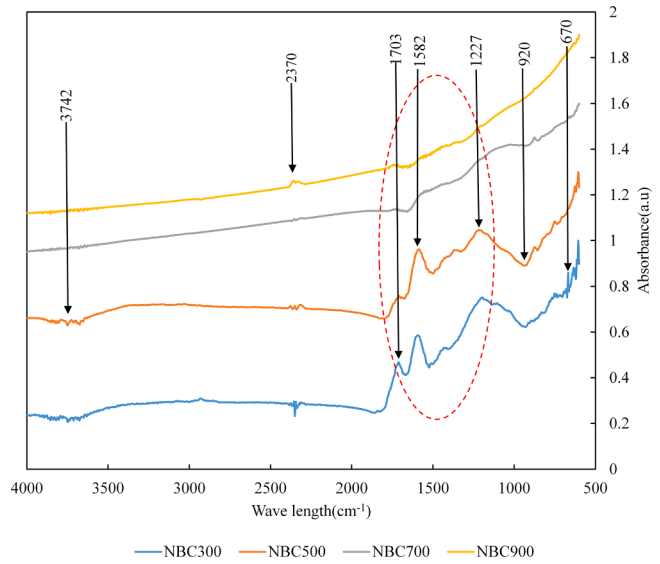

Fig. 3. FTIR analysis of biochar produced at different temperatures

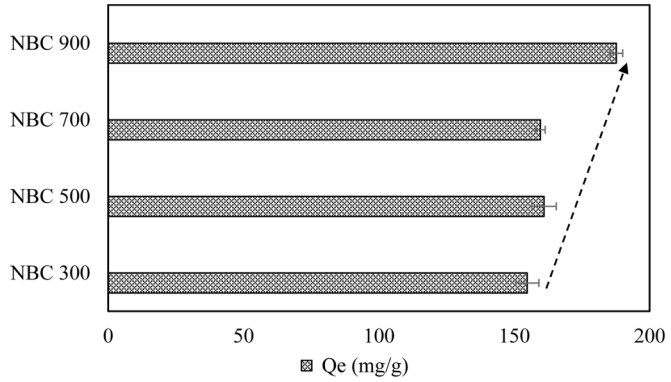

Fig. 4. Adsorptive experiment of different biochars (pH - 5, temperature - 25°C, initial concentration - 200 mg/L).

(Tran et al., 2016). The pzc plays a major role in determining the optimum pH for adsorptive experiments.

3.1.3. Carbon structure

Fig. 2 illustrates the XRD pattern of neem chip biochar pyrolyzed at different temperatures 300, 500, 700 and 900 °C. The structural and chemical compositions of biochar are depicted in the XRD analysis. The XRD was used to identify crystalline components in the samples utilizing prominent peaks describing potential minerals present in the resultant biochar (Zhang et al. 2018b). The XRD spectrum revealed many peaks, confirming the development of a huge range of mineral crystals and other inorganic components during pyrolysis process. The XRD patterns of the major peaks at 2 theta values, 29.36°, 39.11°, 43.13°and 48.4° of biochars, NBC500, NBC700 and NBC900, were almost similar to each other. In these biochar samples, the wide peak in the the range of 2 theta value from 20° to 30° indicates the early presence of poor crystalline structure and carbon-rich phase in these biochar, and the intensity of wider peak decreases as pyrolysis temperature increases confirming the breakdown of cellulose and other structural composition as stated by Zhang et al. (2018a)

No strongest peak was formed for NBC300. In addition to NBC500, the strongest peak was formed at 2 theta of 29.21° along with remarkable shallow peaks at 2 theta of 35.86°, 41.47°, 42.99°, 47.29° and 48.19°. Furthermore, for NBC700, the strongest peak obtained at 2 theta of 28.77 along with remarkable shallow peaks at 35.23°, 38.84°, 41.43°,

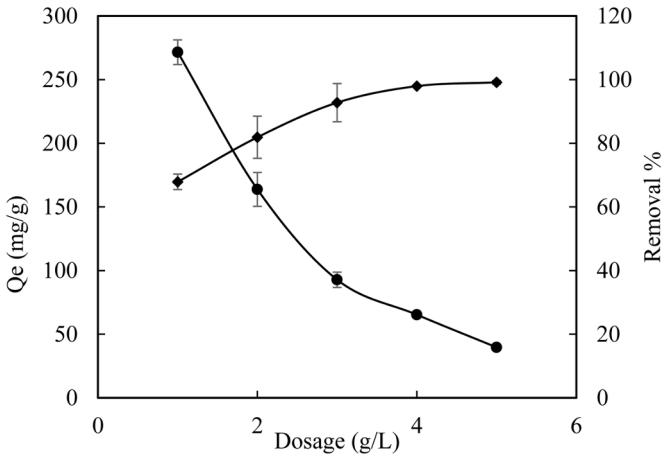

Fig. 5. Effect of NBC900 dosage on mancozeb adsorption (pH - 5, temperature -25°C, initial concentration - 200 mg/L).

42.61°, 47.03° and 47.95°. In addition, for NBC900 the strongest peak observed at the 2 theat of 29.36° along with remarkable shallow peaks at 2 theta of 22.96°, 35.97°, 39.36°, 41.33°, 47.43°, 48.45°, 57.36° and 83.34°. Various new peaks were observed for NBC900. The strong peak formed at the 2 theta of 29.11° indicates the presence of pyrophyllite. Several new peaks formed at NBC900 indicate the formation of new compounds due to degradation and higher pyrolysis temperature (Waqas et al., 2018). Furthermore, shallow peaks at 2 theta of 39.1° and 43.13° are indicating the presence of gibbsite and hydrobiotite. Also, peaks at 2 theta of 28° and 40° indicate the presence of mineral crystals like $CaCO_3$ and Na_4SiO_4 in neem biochar samples (Zhang et al., 2018a). The composition of mineral compounds and other organic compounds are less as no significant peaks were appeared at 300 °C during biochar production. The amount of mineralogical composition of biochar increases with an increase in pyrolysis temperature.

3.1.4. Surface functional group

The FTIR spectra of different biochars pyrolyzed at different temperatures of 300, 500, 700 and 900 °C are given in the Fig. 3. Significant changes can be observed with increasing temperature. Common peaks like 1227, 1582 and 1703 cm-1were observed in both spectra obtained from NBC300 and NBC500. Spectra for NBC300 and NBC500 are almost same. With the increase in temperature, formation of remarkable peak is getting decreased. Significant changes can be observed in the band region, 1212 - 1853 cm^{-1}. This indicates the bands correlated with oxygen containing functional groups like carbonyl and alcoholic –OH stretching get decreased with increasing temperature. The band region of 1302 and

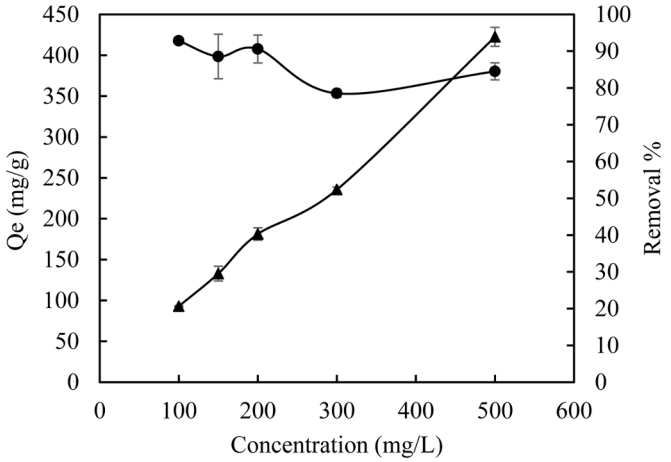

Fig. 6. Effect of initial concentration in adsorption to NBC 900.

Table 1
Kinetics parameters of mancozeb adsorption by NBC900.

Ci (mg/L)	Pseudo first order				Pseudo second order				Elovich		
	q_e.cal.(mg/g)	q_e.exp.(mg/g)	K_1	R^2	q_e.cal.(mg/g)	qe.exp.(mg/g)	K_2	R^2	α	β	R^2
100	12.314	96.870	0.002	0.360	98.039	96.8700	0.0011	0.9992	6781.123	0.1374	0.5012
300	117.766	285.544	0.003	0.940	294.118	285.5440	0.0000	0.9869	12351.242	0.0535	0.2680
500	131.894	422.056	0.003	0.905	416.667	422.0560	0.0001	0.9990	1200.094	0.0234	0.7893

1706 cm $^{-1}$ indicates the presence of organic residues and carboxyl functional groups (Nadarajah et al., 2021) on the surface of biochar pyrolyzed at 300 and 500 °C. The amount of these groups decreased with temperature. The spectra demonstrated a continuous loss of aromatic groups until the dominance of graphitic C in the upper temperature range of 700 - 900 °C (Liu et al., 2015). The strong band at 1000 cm^{-1} indicates the presence of C-O stretching caused by the hemicellulosic groups like quinine and lactone. The intensity of C-O stretching decrease with an increase in pyrolysis temperature, indicating the breakdown of hemicellulosic components at higher temperature. There is an evidence reported by Waqas et al.,(2018), indicating that the increase in pyrolysis temperature causes a reduction in carboxylic acid and degradation of hemicellulosic components.

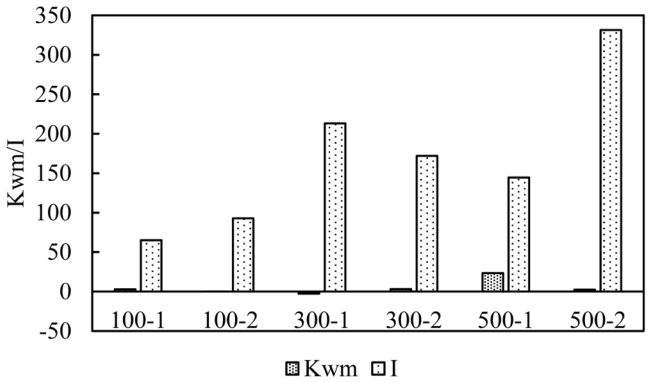

Fig. 7. Relationship between Kwm/I and initial concentration.

3.2. Adsorption experiment

Fig. 4 shows the adsorptive performances of biochar pyrolyzed at different temperatures (NBC300, NBC500, NBC700 and NBC900) for mancozeb. Different biochars pyrolyzed at different temperatures exhibit various adsorptive performance as shown in Fig. 4 due to the variations in surface functional properties like constricted carbon structure and functional groups. Qe values (mg/g) of NBC300, NBC500, NBC700 and NBC900 are 154.794, 161.003, 159.637 and 187.68 mg/g respectively. The Qe values (mg/g) for NBC500 and NBC700 were approximately similar, and the Qe value (mg/g) for NBC900 exhibited higher value of 187.68 mg/L. In addition, NBC300 expressed the lowest adsorptive performance compared to other biochars. Biochar pyrolyzed at 900 °C exhibited excellent adsorptive performance in terms of mg/g and removal percentage because of its enhanced carbon network compared to other biochars.

It has been reported that surface area and development of constricted carbon structure had a linear relationship with pyrolysis temperature. The increased pore volume and surface area are caused due to the thermal degradation of organic materials and occurrences of channel structure during pyrolysis. Furthermore, degradation of lignin in higher pyrolysis temperature is responsible for the formation of H_2 and CH_4 which lead to the rapid increase in surface area and pore volume (Chatterjee et al., 2020). Biochar produced at 900 °C from neem chips (NBC900) was considered for detailed study due to its enhanced performance (isotherm, kinetics and thermodynamics). The adsorption of mancozeb with biochar during adsorptive process is mainly via hydrophobic interaction and mass diffusion of molecules. Hence, a reasonable temperature can be taken for pyrolysis of neem chips for having enhanced surface functional properties required for better removal of mancozeb.

3.3. Factors influence the removal of mancozeb

3.3.1. Dosage

Fig. 5 shows changes in the adsorptive performance of NBC900 with different biochar dosages. The adsorptive performance Qe (mg/L) was reduced with an increase in absorbent dosage. The Qe values of NBC900 at adsorptive dosages of 0.5 g/L, 1 g/L, 2 g/L, 3 g/L and 5 g/L are 271.53, 163.78, 92.77, 63.30 and 39.67 mg/g respectively. As dosage increases, there is the possibility to have increased surface sites on the biochar. However, the removal performance reduces due to the limited availability of mancozeb in the adsorptive system. The removal performance in percentage is different from this scenario as it is referred to the initial concentration only. It is possible to have high removal performance in percentage as the dosage is high. Hence, by considering this hydrophobic interaction, an optimum dosage of NBC900 could be selected for the removal of mancozb. That is 5 g/L based on the above discussion. Furthermore, the higher adsorptive performance of mancozeb was due to the availability of higher mass of NBC900, which

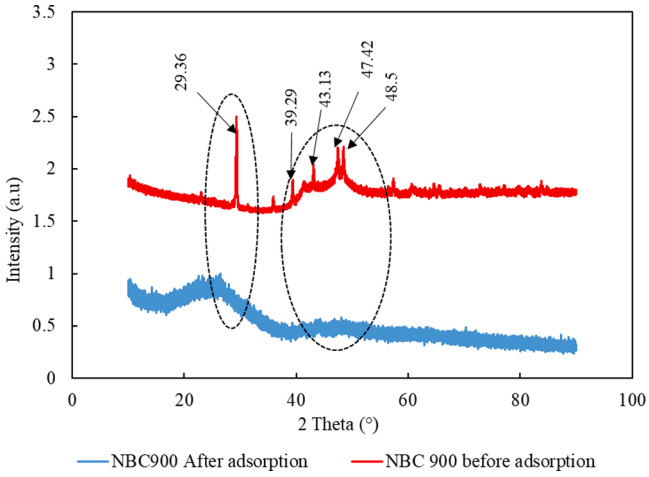

Fig. 8. XRD spectrum before and after adsorption by mancozeb

Table 2
Parameters of Langmuir, Freundlich and Temkin models.

Contaminant	Langmuir			Freundlich			Temkin		
	q_m	K_L	R^2	1/n	K_f	R^2	A_t	b_t	R^2
Mancozeb	500	0.03	0.69	0.54	31.67	0.89	3.93	2.19	0.77

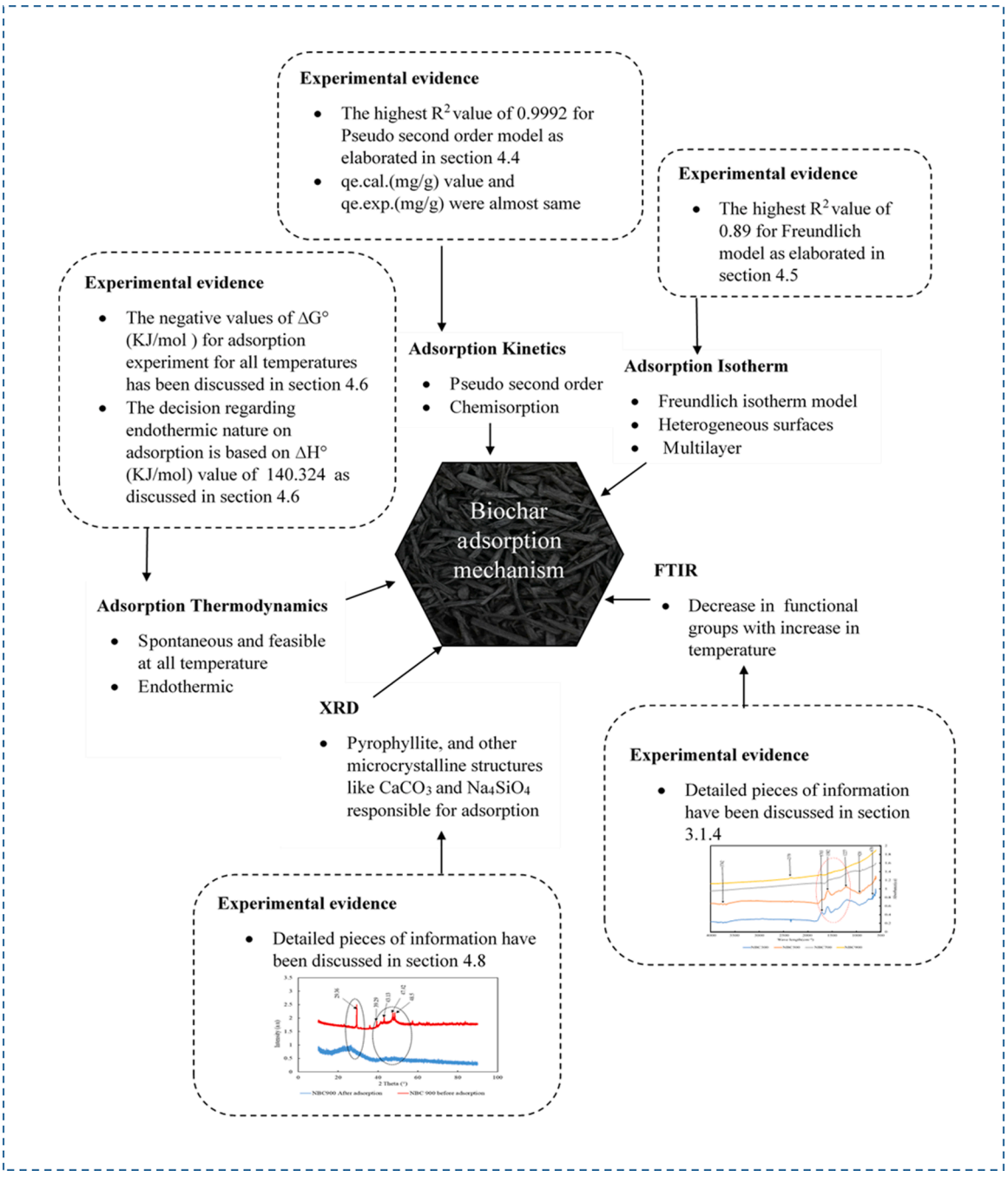

Fig. 9. Adsorption mechanism.

facilitates the formation of effective attractive force for better adsorption (Nadarajah et al., 2021). In addition, higher dosage of biochar exhibits higher adsorption surface area and higher adsorption sides (Jia et al., 2018). Thus, the removal efficiency of 99.41% was obtained for the dosage of 5 g/L.

3.3.2. *Initial concentration*

Fig. 6 describes the effect of the initial concentration of mancozeb on the adsorptive performance of NBC900 at 25 °C with a dosage of 1 g/L and pH at 5. The adsorptive performances in terms of Qe (mg/g) increase with an increase in initial concentration of mancozeb. The Qe values of NBC900 at dosage of 1 g/L temperature at 25 °C and pH of 5 with the initial concentrations of 100, 150, 200, 300 and 500 mg/L are 92.85, 132.86, 181.22, 235.62 and 422.5 mg/g respectively. This matches with the previous study which was conducted using Switchgrass biochar produced from fast pyrolysis for the removal of phenoxy herbicides, 2,4-D and MCPA. They reported that the adsorption capacity (Qe in mg/g) increases with initial concentration (Essandoh et al., 2017). An increasing trend in the study of heavy metal removal using hydrochar due to the high chance of contact with molecules in high concentrations has also been repored (Nadarajah et al., 2021).

In contrast, removal percentages show a decreasing trend with increasing concentration. This might be due to the increased numbers of mancozeb molecules than the numbers of active sites of biochar as the dosage is constant for all initial concentrations (Keerthanan et al., 2020). The removal percentages for 100, 150, 200, 300 and 500 mg/L are 92.85, 88.57, 90.61, 78.54 and 84.5 respectively.

3.3.3. pH

The effect of pH on the removal of mancozeb by NBC900 is illustrated in Fig. S3. the pH plays a major role in adsorptive performance. The pH assay experiment was carried out with macozeb with an initial concentration of 200 mg/L, a dosage of 1 g/L and at 25 °C. The pH range from 3 to 11 was used. Higher adsorptive performance of mancozeb was achieved at the pH of 11, whereas lower performance was observed at the pH of 4. Above the pH of 9, the Q_e values are almost same. Many properties of biochar such as capacity to capture particles, extent of ionization and surface functional groups are influenced by pH (Nworie et al., 2019). The pzc value of NBC900 is 10.1 as indicated by Fig. 1 above. At the pH below pzc value, the surface of biochar is positively charged to cause repulsion with mancozeb molecules, and it reduces the removal of mancozeb from solution. When the pH of the solution approaches pzc value, the biochar is negatively charged and increases the interaction with mancozeb molecules for better removal. At basic pH, there is a decrease in the number of positive sites and an increase in negative charges, resulting in greater removal of mancozeb (Nworie et al., 2019).

4.4. Adsorption kinetics

The kinetic study was carried out for mancozeb with different initial concentrations of 100, 300 and 500 mg/L. Three different kinetic models (Pseudo first order, Pseudo second order and Elovich) were used to explain the mancozeb adsorption by NBC900. The results obtained after implementing Pseudo first order, Pseudo second order and Elovich models for fitting the outcomes of mancozeb adsorption by NBC900 are tabulated in Table 1. R^2 values obtained from linear regression and other parameters like K_1, K_2, α and β obtained from the respective graphs plotted for each model are given in supplementary information (Figs. S4-S6). R^2 values obtained from the Pseudo second order model are almost 0.99 for all concentrations. Compared to Pseudo first order and Elovich models, Pseudo second order model is considered to have high correlation values. To gain a better understanding of the adsorption process, Pseudo second order analysis is used, which is devoid of the impact of equilibrium concentration. As of chemisorption during metal ion adsorption, it takes longer to reach equilibrium and results in a poor match for the kinetic study (Nadarajah et al., 2021). The higher R^2 values indicates that the equilibrium concentration plays a major role in the removal rate of mancozeb and also confirms that there is an influence of chemisorption during the adsorption process. In addition, the calculated q_e (q_e.cal) values were more or less similar to the experimental q_e ($q_{e.}$exp) values in Pseudo second order model. Therefore, based on the above discussion, the Pseudo second order is a well fitted model which describes the kinetics of mancozeb adsorption process by NBC900 and the adsorption process is influenced by the chemisorption (Nadarajah et al., 2021).

4.5. Adsorption isotherm

Adsorptive isotherm was carried out using the data of the effect of the initial concentrations, 100, 200, 300 and 500 mg/L, of mancozeb, on adsorption as described previously in Fig. 6. Three different models, Langmuir, Freundlich and Temkin, were used to study the sorption capacity, heat of sorption and adsorption intensity respectively for NBC900. The results obtained after implementing Langmuir, Freundlich and Temkin models for fitting the outcomes of mancozeb adsorption by NBC900 are tabulated in Table 2. The R^2 values were obtained from linear regression and other parameters like Q_m, n, A_t and b_t were obtained from the respective graphs plotted for each model illustrated in the supplementary information (Figs. S7-S9).

The Langmuir model is an appropriate adsorption model for the monolayer adsorption which means that every site of the adsorption surface has equal adsorption energies. The Freundlich model is ideal for adsorption to heterogeneous surfaces and it continues to improve its absorption potential at high concentrations. The Temkin model assumes that the adsorption heat decreases linearly with the intensity of absorbate and adsorbent interaction (Wu et al., 2019). Data that belong to Freundlich model exhibit the highest overall regression coefficient and better fit than other two models. The R^2 value for Freundlich model is 0.8853. Moreover, the coefficient of heterogeneity (1/n) of Freundlich model is 0.544. It falls between 0 and 1 indicating the adsorption process is favorable (Van Hien et al., 2020). Based on this above discussion, adsorption of NBC900 is well fitted with Freundlich isotherm model, and it further indicates that the adsorption occurs on heterogeneous surfaces with multilayer mode (Wu et al., 2019).

4.6. Adsorption thermodynamics

An adsorption thermodynamic study was carried out to examine the effect of temperature on the adsorptive performance on NBC900 and to find out whether the adsorption is spontaneous and endothermic in nature. It was carried out with three different temperatures, 25, 30 and 40 °C. Thermodynamic parameters, ΔH° and ΔS°, were determined from slope and intercept of graph given in Fig. S10. Thermodynamic parameters of mancozeb adsorption are given in Table S1. The changes in Gibbs free energy (ΔG°) is decided by both enthalpy and entropy factors. It determines spontaneous nature of adsorption and reaction feasibility (Vithanage et al., 2016). Negative ΔG° indicates that the reaction is spontaneous at a given temperature. The ΔG° values at 25, 30 and 40 °C are -11.005, -13.544 and -18.622 kJ/mol respectively. All of the ΔG° values were negative, confirming that mancozeb adsorption onto neem biochar was spontaneous and feasible at all temperatures (Vithanage et al., 2016).

Enthalpy change (ΔH°) is a measure of the energy changes that arise as a result of adsorbate interaction. The enthalpy change of mancozeb was 140.324 kJ/mol, indicating the adsorption reaction is endothermic. The entropy change (ΔS°) measures the binding or repulsive forces in the system and it is associated with spatial arrangement of the adsorbate - adsorbent interface. The entropy change (ΔS°) of mancozeb was 0.508 kJ/mol K. The positive value of ΔS° indicates the affinity of NBC900 and describes the structural changes of NBC900 during the adsorption process (Vithanage et al., 2016).

4.7. Rate limiting analysis

Rate limiting factor analysis was done using the data obtained from the kinetics study. The study of rate limiting is vital to understand the movement of compounds onto the surface and into the pore spaces of biochar. It also helps to understand the rate limiting process during adsorption. Weber-Morris model was used to investigate rate limiting factor. The linear plot of qt Vs $\sqrt{t}$ is illustrated in Fig. S11. Kwm (inter particle diffusion rate) and I (Thickness of boundary layer) were obtained from the slope and intercept respectively for three different concentrations. The relationship between Kwm/I and initial concentration is shown in Fig. 7 . The Weber-Morris study revealed two distinct phases for mancozeb adsorption. The first linear phase of the q_t vs $\sqrt{t}$ plot reflects mass movement of mancozeb from the solution into the surface of the biochar, while the second linear portion represents the movement of mancozeb particles through the biochar's surface and internal openings. In addition, higher slope of phase 1 for 100 and 500 mg/L indicates rapid movement of mancozeb particles to the outer surface of biochar. This is due to the rapid movement of mancozeb particles as of the attractive forces developed by functional groups (Nadarajah et al., 2021). Lower slope of phase 2 for 100 mg/L and 500 mg/L indicates the influence of intraparticle diffusion after a long reaction period.

4.8. XRD spectra

The XRD pattern of NBC900 before and after adsorption of mancozeb is illustrated in Fig. 8. Remarkable peaks at 2 theta of 29.36°, 39.29°, 43.13°, 47.42° and 48.5° obtained for NBC900 before adsorption are getting reduced due to the adsorption of mancozeb. The signal changes indicate the pyrophyllite, and other microcrystalline structures like $CaCO_3$ and Na_4SiO_4 are responsible for adsorption process. The reduction of peaks may be due to the interaction of minerals and organic components like pyrophyllite, gibbsite, $CaCO_3$, Na_4SiO_4 and hydrobiotite with mancozeb during adsorption process.

5. Conclusion

The detailed scientific investigation of biochar derived from neem chips for the removal of emerging contaminant, mancozeb, yielded interesting outcomes for the development of effective removal strategies at lowest cost of production compared to sophisticated strategies currently used. It is an encouraging study to have further modifications to reach commercial level removal performances. The biochar pyrolyzed at 900 °C expressed the highest q_e value of 187.68 mg/g for mancozeb as of increased mineral components and constricted carbon network. These functional properties of biochar are highly important for the better removal of mancozeb from the aqueous phase. Isotherm analysis indicated that the Freundlich model is well fitted and could explain the nature of adsorption of mancozeb by NBC900. It further explains that the adsorption is multilayer in nature, and it occurs on heterogeneous sites of the NBC900. In kinetic study, Pseudo second order model was well fitted with analyzed data. It explains the adsorption rate and clearly emphasized the involvement of chemisorption process in the removal of mancozeb by the NBC900. The equilibrium is attained after 2 h of the adsorptive process. The adsorption process of mancozeb by the NBC900 is spontaneous and endothermic. Therefore, this information is highly useful in determining the optimum temperature and arrangements needed for the better removal of mancozeb from the aqueous phase. The complete graphical adsorption mechanism of the novel NBC900 is given in Fig. 9.

Declaration of Competing Interest

The authors declare that they have no known competing financial interests or personal relationships that could have appeared to influence the work reported in this paper.

CRediT authorship contribution statement

Thusalini Manoharan: Investigation, Data curation, Writing – original draft. Sashikesh Ganeshalingam: FTIR analysis. Kannan Nadarajah: Conceptualization, Data curation, Writing – review & editing, Project administration.

Acknowledgment

The authors would like to acknowledge Department of Agricultural Engineering, Faculty of Agriculture, University of Jaffna Sri Lanka for proving the necessary facilities to undertake this study. We would also like to thank Department of Civil Engineering, Faculty of Engineering, University of Jaffna for proving instrument support. Technical assistance for XRD analysis was provided by Dr.M.Thanihaichelvan, Department of Physics, Faculty of Science, University of Jaffna.

Supplementary materials

Supplementary material associated with this article can be found, in the online version, at doi:10.1016/j.envadv.2021.100158.

References

Al-Eraky, M.M., Mohamed, N., Kamel, F., Al-Qahtani, A., Madini, M.A., Hussin, A., Kamel, N.M.F., 2016. Teaching professionalism by vignettes in psychiatry for nursing students. Int. J. Adv. Res. 4, 625–634.
Al-Wabel, M.I., Al-Omran, A., El-Naggar, A.H., Nadeem, M., Usman, A.R.A., 2013. Pyrolysis temperature induced changes in characteristics and chemical composition of biochar produced from conocarpus wastes. Bioresour. Technol. 131, 374–379.
Angelo, G., Gregory, M.K., Leonardo, B., Brian, S., 2010. History and role of mancozeb in disease management. Plant Dis. 94, 1076–1087.
Banik, C., Lawrinenko, M., Bakshi, S., Laird, D.A., 2018. Impact of pyrolysis temperature and feedstock on surface charge and functional group chemistry of biochars. J. Environ. Qual. 47, 452–461.
Bhattacharyya, K.G., Sharma, A., 2004. Adsorption of Pb(II) from aqueous solution by Azadirachta indica (Neem) leaf powder. J. Hazard. Mater. 113, 97–109.
Bhattacharyya, K.G., Sharma, A., 2005. Kinetics and thermodynamics of methylene blue adsorption on neem (azadirachta indica) leaf powder. Dyes Pigment 65, 51–59.
Chatterjee, R., Sajjadi, B., Chen, W.Y., Mattern, D.L., Hammer, N., Raman, V., Dorris, A., 2020. Effect of pyrolysis temperature on physicochemical properties and acoustic-based amination of biochar for efficient CO_2 Adsorption. Front. Energy Res. 8, 1–18.
Essandoh, M., Wolgemuth, D., Pittman, C.U., Mohan, D., Mlsna, T., 2017. Phenoxy herbicide removal from aqueous solutions using fast pyrolysis switchgrass biochar. Chemosphere 174, 49–57.
FAOSTAT. (2021), "Pesticide use", Food and Agriculture Organization of the United Nations, available at: https://www.fao.org/3/cb3411en/cb3411en.pdf (accessed 14 August 2021).
Homem, V., Santos, L., 2011. Degradation and removal methods of antibiotics from aqueous matrices-a review. J. Environ. Manag. 92, 2304–2347.
Jia, Y., Shi, S., Liu, J., Su, S., Liang, Q., Zeng, X., Li, T., 2018. Study of the effect of pyrolysis temperature on the Cd2+ adsorption characteristics of biochar. Applied Sciences (Switzerland) 8 (7), 1–14.
Keerthanan, S., Rajapaksha, S.M., Trakal, L., Vithanage, M., 2020. Caffeine removal by Gliricidia sepium biochar: Influence of pyrolysis temperature and physicochemical properties. Environmental Research 189, 109865.
Khan, N.A., Khan, S.U., Ahmed, S., Farooqi, I.H., Yousefi, M., Mohammadi, A.A., Changani, F., 2020. Recent trends in disposal and treatment technologies of emerging-pollutants-a critical review. TrAC Trends Anal. Chem. 122, 115744.
Li, L., Zou, D., Xiao, Z., Zeng, X., Zhang, L., Jiang, L., Wang, A., Ge, D., Zhang, G., Liu, F., 2019. Biochar as a sorbent for emerging contaminants enables improvements in waste management and sustainable resource use. J. Clean. Prod. 210, 1324–1342.
Liu, Y., He, Z., Uchimiya, M., 2015. Comparison of biochar formation from various agricultural by-products using FTIR spectroscopy. Mod. Appl. Sci. 9, 246–253.
Mandal, A., Bar, N., Das, S.K., 2020. Phenol removal from wastewater using low-cost natural bioadsorbent neem (Azadirachta indica) leaves: adsorption study and MLR modeling. Sustain. Chem. Pharm. 17, 100308.
MarketWatch News Department, 2021. Mancozeb Market 2021 Growth Analysis, Share, and consumption by Regional data, Investigation and Growth, Demand by Regions, Types and Analysis of Key Players- Research Forecasts To 2026 [WWW Document]. News Dep., Mark.
Matamoros, V., Salvadó, V., 2013. Evaluation of a coagulation/flocculation-lamellar clarifier and filtration-UV-chlorination reactor for removing emerging contaminants at full-scale wastewater treatment plants in Spain. J. Environ. Manag. 117, 96–102.
Nadarajah, K., Bandala, E.R., Zhang, Z., Mundree, S., Goonetilleke, A., 2021. Removal of heavy metals from water using engineered hydrochar: kinetics and mechanistic approach. J. Water Process Eng. 40, 101929.
Naidu, R., Arias Espana, V.A., Liu, Y., Jit, J., 2016. Emerging contaminants in the environment: risk-based analysis for better management. Chemosphere 154, 350–357.
Naiya, T.K., Bhattacharya, A.K., Das, S.K., 2008. Adsorption of Pb(II) by sawdust and neem bark from aqueous solutions. Environ. Prog. 27, 313–328.
Novak, J., Lima, I., Xing, B., Gaskin, J., Steiner, C., Das, K., Ahmedna, M., Rehrah, D., Watts, D., Busscher, W., 2009. Characterization of designer biochar produced at different temperatures and their effects on a loamy sand. Ann. Environ. Sci. 3, 195–206.
Nworie, F.S., Nwabue, F.I., Oti, W., Mbam, E., Nwali, B.U., 2019. Removal of methylene blue from aqueous solution using activated rice husk biochar: Adsorption isotherms, kinetics and error analysis. J. Chil. Chem. Soc. 64, 4365–4376.
Petha, N.H., Lokhande, R.S., Seshadri, D.T., Patil, R.M., Bhagat, T.S., Patil, J.G., 2017. A simple pre-column derivatization method for the determination of mancozeb technical (fungicide) by reverse phase HPLC-UV. Anal. Methods 9, 4702–4708.
Rodriguez-Narvaez, O.M., Peralta-Hernandez, J.M., Goonetilleke, A., Bandala, E.R., 2017. Treatment technologies for emerging contaminants in water: A review. Chemical Engineering Journal 323, 361–380.
Rosenfeld, P.E., Feng, L.G.H., 2011. Emerging Contaminants. Feng, L.G.H.B.T.-R. of H. W.. In: Rosenfeld, P.E. (Ed.), Risks of Hazardous Wastes. William Andrew Publishing, Boston, pp. 215–222.
Runkle, J., Flocks, J., Economos, J., Dunlop, A.L., 2017. A systematic review of Mancozeb as a reproductive and developmental hazard. Environ. Int. 99, 29–42.
Shinogi, Y., Kanri, Y., 2003. Pyrolysis of plant, animal and human waste: Physical and chemical characterization of the pyrolytic products. Bioresour. Technol. 90, 241–247.
Thangagiri, B., Sakthivel, A., Jeyasubramanian, K., Seenivasan, S., Dhaveethu Raja, J., Yun, K., 2022. Removal of hexavalent chromium by biochar derived from Azadirachta indica leaves: batch and column studies. Chemosphere 286, 131598.

Tran, H.N., You, S.J., Chao, H.P., 2016. Effect of pyrolysis temperatures and times on the adsorption of cadmium onto orange peel derived biochar. Waste Manag. Res. 34, 129–138.
Van Hien, N., Valsami-Jones, E., Vinh, N.C., Phu, T.T., Tam, N.T.T., Lynch, I., 2020. Effectiveness of different biochar in aqueous zinc removal: Correlation with physicochemical characteristics. Bioresource Technology Reports 11, 100466.
Vithanage, M., Mayakaduwa, S.S., Herath, I., Ok, Y.S., Mohan, D., 2016. Kinetics, thermodynamics and mechanistic studies of carbofuran removal using biochars from tea waste and rice husks. Chemosphere 150, 781–789.
Waqas, M., Aburiazaiza, A.S., Miandad, R., Rehan, M., Barakat, M.A., Nizami, A.S., 2018. Development of biochar as fuel and catalyst in energy recovery technologies. J. Clean. Prod. 188, 477–488.
da S.R. Weis, G.C.C., Assmann, C.E., Cadoná, F.C., Bonadiman, B, Alves, A.O., Machado, A.K., Duarte, M.M.M.F., da Cruz, I.B.M., Costabeber, I.H., 2019. Immunomodulatory effect of mancozeb, chlorothalonil, and thiophanate methyl pesticides on macrophage cells Ecotoxicol. Environ. Saf. 182, 109420.
Wu, Q., Xian, Y., He, Z., Zhang, Q., Wu, J., Yang, G., Zhang, X., Qi, H., Ma, J., Xiao, Y., Long, L., 2019. Adsorption characteristics of Pb(II) using biochar derived from spent mushroom substrate. Sci. Rep. 9, 1–11.
Zhang, J., Huang, B., Chen, L., Du, J., Li, W., Luo, Z., 2018a. Pyrolysis kinetics of hulless barley straw using the distributed activation energy model (DAEM) by the TG/DTA technique and SEM/XRD characterizations for hulless barley straw derived biochar. Braz. J. Chem. Eng. 35, 1039–1050.
Zhang, J., Huang, B., Chen, L., Li, Y., Li, W., Luo, Z., 2018b. Characteristics of biochar produced from yak manure at different pyrolysis temperatures and its effects on the yield and growth of highland barley. Chem. Speciat. Bioavailab. 30, 57–67.